DYNAMIC TRIANGULATION FOR MOBILE ROBOT LOCALIZATION USING AN ANGULAR STATE KALMAN FILTER

Josep Maria Font, Joaquim A. Batlle

Department of Mechanical Engineering
Technical University of Catalonia (UPC)
Avda. Diagonal 647, 08028 Barcelona, Catalonia, Spain
{josep.m.font, agullo.batlle}@upc.edu

ABSTRACT

Localization is one of the fundamental problems in mobile robot navigation. Several approaches to cope with the dynamic positioning problem have been made. Most of them use an extended Kalman filter (EKF) to estimate the robot configuration –position and orientation– fusing both the robot odometry and external measurements. In this paper, an EKF is applied to estimate the angles, relative to the robot frame, of the straight lines from a rotating laser scanner to a set of landmarks. By means of these angles, triangulation can be consistently applied at any time to determine the robot configuration. The method is robust to outliers because an expected value of each landmark angle is determined at any time. Simulation and experimental results showing the accuracy of this method are presented.

1. INTRODUCTION

Mobile robots are increasingly used in flexible manufacturing industry and service environments. The main advantage of these vehicles is that they can operate autonomously in their workspace. To achieve this automation, mobile robots must include a localization –or positioning– system in order to estimate the robot configuration –position and orientation– as accurately as possible [1]. In the past two decades, a number of different approaches have been proposed to solve the localization problem. These can be classified into two groups [2]: relative and absolute localization methods.

In relative localization, dead reckoning methods –odometry and inertial navigation– are used to calculate the robot position and orientation from a known initial configuration. Odometry is a widely used localization method because of its low cost, high updating rate, and reasonable short path accuracy. However, its unbounded growth of time integration errors with the distance travelled by the robot is unavoidable and represents a significant inconvenience [3]. Several approaches have been done to cope with the odometry error propagation [4], [5].

Conversely, absolute localization methods estimate the robot position and orientation by detecting distinct features of a known environment. Most of the work published integrates a prediction phase, based on the odometric data and the robot kinematics, and a correction –or estimation– phase that takes into account external measurements. The most used methods are based on Kalman filtering [6], [7], [8] and Bayesian localization [9], [10]. Bayesian localization methods are robust to complex, dynamic and badly mapped environments, but are in general less accurate. Finally, other authors deal with absolute localization using bounded-error state estimation applying interval analysis such in [11].

In this paper, an extended Kalman filter (EKF) is used to estimate in real time the angles –relative to the robot frame– of the straight lines from the sensor (a rotating laser scanner in this case) to the landmarks. Then, by means of triangulation, which refers to any process which solves a system of simultaneous algebraic or transcendental equations –whether or not they are reducible to an equivalent problem involving triangles– [12], the robot localization can be consistently determined at any time.

In mobile robotics, triangulation occurs often in the context of artificial landmarks. However, any natural aspects of the environment –such as walls or corners– whose positions are known, and are detected by a sensor whose indications depend on their position relative to the sensor, establish a triangulation context. This approach is an extension of the method presented in [13], in which the odometry and laser sensor errors were not taken into account.

In section 2, the triangulation methods for mobile robot localization and their properties are described. Next, vehicle kinematics and the expressions for the angular state odometry are reported to introduce the dynamic state estimator, which is presented in section 4. In sections 5 and 6, computer simulations and experimental results showing the positioning accuracy of the presented method, compared to other existing localization approaches, are reported.

2. TRIANGULATION BASED MOBILE ROBOT LOCALIZATION

By means of triangulation it is possible to determine the robot position and orientation from the landmarks position and the measured angles θ_1, θ_2 and θ_3 –relative to the robot longitudinal axis– for three of them (Fig. 1) [14], [15]. As the accuracy of triangulation algorithms depends upon the point of observation and the landmark arrangements [14], more than three landmarks can also be used to improve the positioning accuracy [16], [17].

In this paper, a laser positioning system has been considered. The main advantage of this system in industrial applications is its high positioning accuracy inside the workspace which is required in certain practical situations such as loading, unloading or narrow crossings. This system consists of a rotating laser scanner and a group of catadioptric landmarks strategically placed.

The laser scanner emits a rotating beam that horizontally sweeps the environment and reflects back when it detects a landmark L_i. The system measures the angle θ_i of the reflected beam, relative to the vehicle longitudinal axis (Fig. 1), by means of an incremental encoder.

For the consistent use of triangulation, the angles θ_i to each landmark must be known at the same mobile robot configuration –position and orientation–. This condition, which is obviously fulfilled under static condition, is not valid under dynamic condition –robot in motion– and therefore triangulation cannot be directly applied because landmarks are detected at different positions and even different orientations of the robot [18].

To solve this problem several authors use recursive algorithms to fuse the robot odometric information and the laser external measurements in order to keep track of the robot configuration. In [7] a Kalman filtering framework is used to fuse this data. Other approaches are based on alternative recursive algorithms that deal with nongaussian noise and deterministic errors [19].

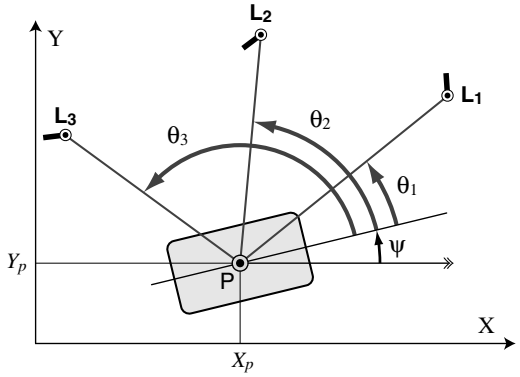

Fig. 1. Mobile robot position and orientation can be calculated from landmarks position and angles θ_1, θ_2, θ_3 by triangulation.

In this paper, to cope with dynamic positioning, an extended Kalman filter –which takes into account the errors associated to odometry and the laser scanner– is used to estimate the relative angles $\theta_i(t)$. Between actual laser measurements angles are predicted by means of the time integration of its time derivative, which depends upon the robot kinematics [13]. Thus, a kind of "angular odometry" substitutes the usual odometry related to the robot pose, and allows the kinematically consistent use of triangulation. The angular state vector used in the EKF is:

$$\boldsymbol{x}_k = \left\{\theta_{1,k}, \theta_{2,k}, ..., \theta_{N,k}\right\}^{\mathrm{T}}, \tag{1}$$

instead of the conventional one $\boldsymbol{x}_k = \{x_k, y_k, \psi_k\}^{\mathrm{T}}$, which is obtained from vector (1) by means of triangulation. In (1) N represents the number of viewed landmarks, in this case $N = 3$.

An additional advantage of the angular odometry developed is that, as it gives an accurate real-time estimation of each angle θ_i, it allows setting a narrow validation gate for each landmark reflection. Angular measurements that do not fall in this validation gate are ignored. If a reflection does not arrive inside the validation gate the angular odometric prediction continues over one more laser revolution. Therefore, the system is robust to possible outliers detected by the laser sensor.

3. VEHICLE KINEMATICS AND ANGULAR ODOMETRY

3.1. Vehicle kinematics

The vehicle studied in this approach is a forklift type mobile robot with a tricycle kinematics. Its main geometric parameters are shown in Fig. 2. The vehicle has

two coaxial wheels located in the fork, the driving and steering wheel, and a castor wheel.

The velocity $\boldsymbol{v}(P)$ of the point P –center of the laser scanner– can be calculated from the velocity v of the center of the driving-steering wheel and its steering angle γ (Fig. 2). Using axes 1-2, $\boldsymbol{v}(P)$ is expressed as:

$$\left\{\boldsymbol{v}\left(P\right)\right\} \equiv \begin{Bmatrix} v_{1p} \\ v_{2p} \end{Bmatrix} = v \begin{Bmatrix} \cos\gamma - \dfrac{p}{L}\sin\gamma \\ \dfrac{L_p}{L}\sin\gamma \end{Bmatrix}, \qquad (2)$$

geometric variables p, L and L_p are defined in Fig. 2. The orientation angle ψ of the robot evolves according to:

$$\dot{\psi} = \frac{v}{L}\sin\gamma\ . \qquad (3)$$

The velocity v and the steering angle γ are known at each time from the driving and steering encoders on the robot.

3.2. Angular odometry

The solution presented to cope with triangulation under dynamic condition is based on the odometric calculation of the evolution of the angle –relative to the vehicle– of the straight lines from the laser scanner (point P) to each landmark L_i.

If ρ_i stands for the distance between point P and the landmark L_i, and θ_i is the angle between the robot longitudinal axis and the straight line from P to this landmark (Fig. 2), the time evolution of θ_i can be expressed, according to the vehicle kinematics, as:

$$\dot{\theta}_i = \frac{\left(v_{1p}\sin\theta_i - v_{2p}\cos\theta_i\right)}{\rho_i} - \dot{\psi}\ . \qquad (4)$$

Discrete time integration of equation (4) determines the evolution of angle θ_i between measurements:

$$\theta_{i,k} = f\left(\theta_{i,k-1}, v_{k-1}, \gamma_{k-1}\right) =$$
$$= \theta_{i,k-1} + \left[\frac{\left(v_{1p,k-1}\sin\theta_{i,k-1} - v_{2p,k-1}\cos\theta_{i,k-1}\right)}{\rho_{i,k-1}} - \dot{\psi}_{k-1}\right]\Delta t\ . \qquad (5)$$

Variable ρ_i can be calculated after estimating the angular state $\boldsymbol{x}_k$ because it is the distance between P, the position of which is determined by angular triangulation, and the landmark L_i.

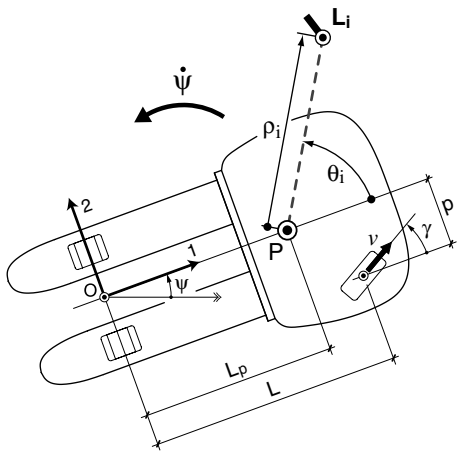

Fig. 2. Geometric and kinematical parameters of the robot. Axes 1 and 2 are body axes.

4. DYNAMIC ANGULAR STATE ESTIMATOR BASED ON KALMAN FILTERING

Kalman filtering is used to estimate at time step k the state vector $\boldsymbol{x}_k$ defined in (1), the dimension of which is the number N of landmarks considered. The nonlinear state transition function used in the EKF describes how the state $\boldsymbol{x}_k$ changes with time in response to a control input $\boldsymbol{u}_k$ and a noise disturbance $\boldsymbol{w}_k$:

$$\boldsymbol{x}_k = \boldsymbol{f}\left(\boldsymbol{x}_{k-1}, \boldsymbol{u}_{k-1}, \boldsymbol{w}_{k-1}\right). \qquad (6)$$

The ith file (i = 1, ..., N) of this transition function $\boldsymbol{f}$, associated to the evolution of angle θ_i, is defined in (5). In the process considered, the control input vector $\boldsymbol{u}_k$ is calculated by the driving and steering encoders at each time step k:

$$\boldsymbol{u}_k = \left\{v_k, \gamma_k\right\}^{\mathrm{T}}. \qquad (7)$$

Noise disturbances in the process model are associated to the measures of input variables v_k and γ_k. These noises are assumed to be gaussian with zero mean and variances σ_v^2 and σ_γ^2 respectively, which have been experimentally determined. The measurement model of the EKF relates the state with the external measure $\boldsymbol{z}_k$ by means of the nonlinear observation function $\boldsymbol{h}$:

$$\boldsymbol{z}_k = \boldsymbol{h}\left(\boldsymbol{x}_k, v_\theta\right), \qquad (8)$$

where $v_\theta \sim N(0,\ \sigma_\theta^2)$ denotes the measurement noise associated to the laser sensor, which also has been experimentally tested. Note that external measures $\boldsymbol{z}_k$ are directly the state of the filter. This fact simplifies the required calculations.

The goal of the state predictor is to produce an estimate of the angular state $\boldsymbol{x}_k$ at time k, based on the estimation $\boldsymbol{x}_{k-1}$ at time step k-1, the control input $\boldsymbol{u}_{k-1}$ and the landmark observation $\boldsymbol{z}_k$ (if any). The algorithm employs the following steps: prediction, observation, matching and estimation.

4.1. Prediction

The first step of the algorithm uses the state transition function (6) to predict the state at time k with the knowledge of $\boldsymbol{u}_{k-1}$:

$$\tilde{\boldsymbol{x}}_k = \boldsymbol{f}\left(\boldsymbol{x}_{k-1}, \boldsymbol{u}_{k-1}, 0\right). \tag{9}$$

Then, the state error covariance associated with this prediction is calculated:

$$\boldsymbol{P}_k^- = \boldsymbol{A}_k \boldsymbol{P}_{k-1} \boldsymbol{A}_k^{\mathrm{T}} + \boldsymbol{W}_k \boldsymbol{Q} \boldsymbol{W}_k^{\mathrm{T}}, \tag{10}$$

where $\boldsymbol{Q}$ is the covariance matrix associated with the noises $\boldsymbol{w}_k$ in the transition function $\boldsymbol{f}$, and matrices $\boldsymbol{A}_k$ and $\boldsymbol{W}_k$ are the jacobians defined by:

$$\boldsymbol{A}_k = \frac{\partial \boldsymbol{f}}{\partial \boldsymbol{x}}\left(\boldsymbol{x}_k, \boldsymbol{u}_k, 0\right),\ \boldsymbol{W}_k = \frac{\partial \boldsymbol{f}}{\partial \boldsymbol{w}}\left(\boldsymbol{x}_k, \boldsymbol{u}_k, 0\right). \tag{11}$$

4.2. Observation and matching

In the following step, an angular measurement arrives and the innovation, which is the difference between the expected angle and the measured one is calculated:

$$\bar{\nu}_k = \boldsymbol{z}_{i,k} - \boldsymbol{h}_i\left(\tilde{\boldsymbol{x}}_k, 0\right) = \theta_{i,k} - \tilde{\theta}_{i,k}. \tag{12}$$

The innovation covariance can be found by linearizing (8) around the prediction:

$$\boldsymbol{S}_k = \boldsymbol{H}_k \boldsymbol{P}_k^- \boldsymbol{H}_k^{\mathrm{T}} + \boldsymbol{V}_k \boldsymbol{R} \boldsymbol{V}_k^{\mathrm{T}}, \tag{13}$$

where $\boldsymbol{R}$ is the covariance matrix associated with the noise v_θ in the laser measurements, and matrices $\boldsymbol{H}_k$ and $\boldsymbol{V}_k$ can be calculated by:

$$\boldsymbol{H}_k = \frac{\partial \boldsymbol{h}}{\partial \boldsymbol{x}}\left(\tilde{\boldsymbol{x}}_k, 0\right),\ \boldsymbol{V}_k = \frac{\partial \boldsymbol{h}}{\partial v_\theta}\left(\tilde{\boldsymbol{x}}_k, 0\right). \tag{14}$$

For each observation, a validation gate is used to decide whether it is accepted or ignored:

$$\bar{\nu}_k\, \boldsymbol{S}_k\, \bar{\nu}_k^{\mathrm{T}} \le g^2. \tag{15}$$

4.3. Estimation

In the last step, the successfully matched observations are used to update the angular state prediction. The Kalman filter gain $\boldsymbol{K}_k$ is calculated to compute the angular state estimation $\boldsymbol{x}_k$, and to update the covariance matrix $\boldsymbol{P}_k$:

$$\boldsymbol{K}_k = \boldsymbol{P}_k^- \boldsymbol{H}_k^{\mathrm{T}} \boldsymbol{S}_k^{-1}, \tag{16}$$

$$\boldsymbol{x}_k = \tilde{\boldsymbol{x}}_k + \boldsymbol{K}_k \bar{\nu}_k, \tag{17}$$

$$\boldsymbol{P}_k = \left(\boldsymbol{I} - \boldsymbol{K}_k \boldsymbol{H}_k\right) \boldsymbol{P}_k^-. \tag{18}$$

5. COMPUTER SIMULATIONS

To illustrate the accuracy of the presented method, several computer simulations have been carried out. A realistic model of the robot motion and the sensors used has been created with *Simulink 6.1* (included in MATLAB R14). By means of this model it is possible to check different localization methods under the same environmental and sensor noise conditions.

Two identical trajectories with the same errors associated to the encoders and laser sensor measures –which have been experimentally modeled– have been performed. The difference between the two simulated trajectories is concerned with the environment, in the first case the robot navigates through a 10 x 6 *m* room, while in the second the dimensions of the workspace are 20 x 12 *m*. The landmark layout in both cases is the same, and the center of the driving-steering wheel follows a 10.3 *m* trajectory –composed of half a circumference and a straight line– at 0.5 ms^{-1}, Fig. 3.

The simulated laser scanner is a real model from *Guidance Control Systems Ltd* that rotates at 8 *Hz* and delivers an accuracy of 0.1 *mrad*. Its maximum reflection distance is 30 *m*.

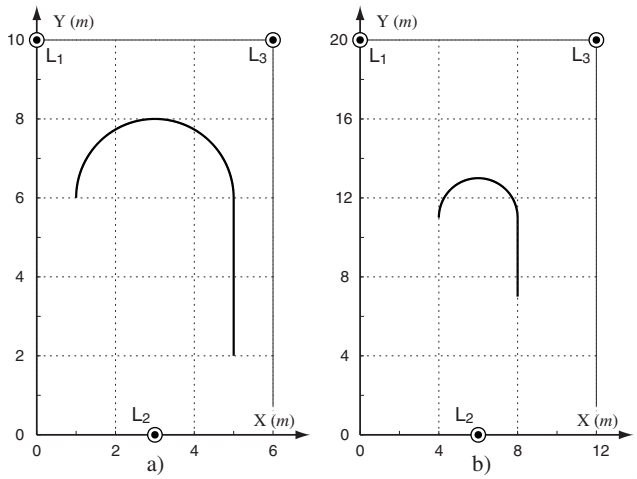

Fig. 3. Simulated trajectories and landmark layout in: a) 10 x 6 *m* environment, and b) 20 x 12 *m* environment.

Tables 1 and 2 show statistical parameters of the lateral error between the actual robot trajectory and the calculated one when using three different approaches: The presented method –angular state EKF and triangulation–, the conventional extended Kalman filter to directly estimate the robot configuration $\{x, y, \psi\}$ from laser measurements without triangulation [7], and the dynamic triangulation method previously presented in [13] –in which the sensor errors were not taken into account–.

Table 1. Comparison between the lateral error (e_{lat}) statistics using different methods (10 x 6 *m* environment)

Localization method	**RMSE** e_{lat} [*mm*]	**mean** $\lvert e_{lat} \rvert$ [*mm*]	**stand. dev.** $\lvert e_{lat} \rvert$ [*mm*]
angular state EKF	0.59	0.54	0.23
EKF $\boldsymbol{x}_k = \{x_k, y_k, \psi_k\}^T$	0.91	0.86	0.29
dynamic triangulation [13]	2.1	1.5	1.4

Table 2. Comparison between the lateral error (e_{lat}) statistics using different methods (20 x 12 *m* environment)

Localization method	**RMSE** e_{lat} [*mm*]	**mean** $\lvert e_{lat} \rvert$ [*mm*]	**stand. dev.** $\lvert e_{lat} \rvert$ [*mm*]
angular state EKF	1.3	1.2	0.51
EKF $\boldsymbol{x}_k = \{x_k, y_k, \psi_k\}^T$	2.2	2.1	0.68
dynamic triangulation [13]	2.8	2.3	1.7

In Tables 1 and 2 the first column indicates the root mean square error of the lateral error, while the others indicate the mean and the standard deviation of the lateral error absolute value respectively. It can be noticed that, under the same conditions, the proposed method performs the best accuracy. Besides this, the standard deviation of the lateral error absolute value is also the lowest, which implies that the results achieved by means of the presented angular state EKF are more reliable.

Another conclusion reached from the results obtained, is that the ratio between the error of the presented angular state EKF and the error of the usual pose state EKF is somewhat smaller when the landmarks are at longer distances. This may be associated with the greater triangulation accuracy near the center of the circumference that contains the three landmarks used.

6. EXPERIMENTAL RESULTS

The method has also been tested on a real forklift mobile robot for industrial applications (Fig. 4a). The robot is provided with the laser scanner described in section 5, and the driving and steering encoders to determine the needed variables v and γ.

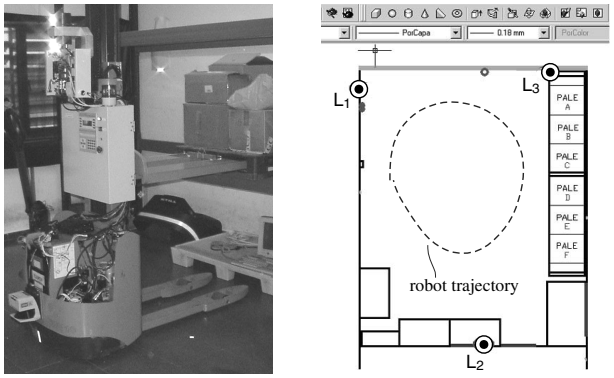

a) b)

Fig. 4. a) Industrial forklift mobile robot used. b) CAD map of the laboratory environment and robot trajectory performed.

The hardware used to support the method is an industrial PC (PC104 based) Pentium III Celeron clocked at 400 *MHz* smartcore. This PC runs with a real-time operative system RT-Linux 3.2. For the odometric and laser signals capture, specific firmware implemented by FPGA is applied.

The robot navigates through the laboratory shown in Fig. 4b, and the same three landmarks (positioned with sub-millimeter accuracy) have been used for all the configurations of the vehicle. In the experiments the robot has been manually guided with a velocity of the driving wheel center in the range of 0.14 – 0.18 ms^{-1}.

To validate the accuracy of the presented method, some points of the actual robot trajectory have been measured using a photometric method based on a high resolution camera [13]. The lateral error e_{lat} between the calculated and the actual points is taken as a measure of the accuracy, and the three methods considered in section 5 are compared under realistic laboratory conditions. Table 3 illustrates the accuracy obtained by means of these methods.

Table 3. Comparison between the lateral error (e_{lat}) statistics using different methods (experimental validation)

Localization method	**RMSE** e_{lat} [*mm*]	**mean** $\lvert e_{lat} \rvert$ [*mm*]	**stand. dev.** $\lvert e_{lat} \rvert$ [*mm*]
angular state EKF	3.8	3.0	2.4
EKF $\boldsymbol{x}_k = \{x_k, y_k, \psi_k\}^T$	6.1	5.4	2.8
dynamic triangulation [13]	6.4	5.0	4.2

It can be seen that the presented angular state Kalman filter reduces the average of the lateral error absolute value from 5 *mm* –achieved by means of the method presented in [13]– to 3 *mm*, which represents a lateral error reduction of 40%. Compared to the pose state EKF, the presented method yields better results also in terms of

positioning accuracy. During the experimental validation, a maximum lateral error of 9.3 *mm* –between the actual and the calculated points– has been obtained when using the presented method.

7. CONCLUSIONS

In this paper, a method to estimate the angles –relative to the robot longitudinal axis– of the straight lines from a laser sensor to a set of landmarks has been presented. This method uses an extended Kalman filter to estimate at each time an angular state vector by fusing the angular odometry –which depends on the robot kinematics– and the laser sensor angular measurements. By means of this discrete time estimator, triangulation can be consistently used at any time to determine the robot configuration –position and orientation–.

The positioning accuracy of this method has been tested by means of computer simulations and by means of experiments using a real forklift prototype –equipped with a laser positioning system, odometric sensors and the required hardware support– navigating through a laboratory environment. The presented approach has been compared to a previous method presented in [13] –in which the odometry and laser sensor errors were not taken into account– and to the conventional use of the EKF to directly estimate the robot pose without applying triangulation. In both, computer simulations and real experiments, the presented approach has turned out to be the best in terms of localization accuracy.

In the future, the method can be improved by using a parameter to evaluate in real time the accuracy of the positioning measurement. This parameter could help to optimise the simultaneous use of more than three landmarks.

Another future line of research is the extension of the presented positioning method to vehicles with kinematics different from that of the tricycle, in particular vehicles with omnidirectional wheels.

8. REFERENCES

[1] Leondes, C. T., *Mechatronic Systems Techniques and Applications Volume 2: Transportation and Vehicular Systems*, Gordon and Breach Science Publishers, Amsterdam, 2000.

[2] J. Borenstein, H. R. Everett, L. Feng and D. Wehe, "Mobile robot positioning – Sensors and techniques", *Journal of Robotic Systems*, Wiley Publishers, vol. 14, no. 4, pp. 231-249, 1997.

[3] A. Kelly, "Linearized error propagation in odometry", *International Journal of Robotics Research*, vol. 23, no. 2, pp. 179-218, 2004.

[4] C. M. Wang, "Location estimation and uncertainty analysis for mobile robots", *Proc. of the IEEE Int. Conference on Robotics and Automation*, Philadelphia, pp. 1230-1235, 1988.

[5] J. Borenstein and L. Feng, "Correction of systematic odometry error in mobile robotics", *Proc. of the IEEE Int. Conf. on Int. Robots and Systems*, Pittsburgh, pp. 569-564, 1995.

[6] J. J. Leonard and H. F. Durrant-Whyte, "Mobile robot localization by tracking geometric beacons", *IEEE Trans. on Robotics and Automation*, vol. 7, no. 3, pp. 376-382, 1991.

[7] H. Hu and D. Gu, "Landmark-based navigation of autonomous robots in industry", *International Journal of Industrial Robot*, Emerald Group Publishing Limited, vol. 27, no. 6, pp. 458-467, 2000.

[8] G. Welch and G. Bishop, "An introduction to the Kalman filter", *Technical Report*, University of North Carolina at Chapel Hill, 2004.

[9] W. Burgard, D. Fox, D. Hennig and T. Schmidt, "Estimating the absolute position of a mobile robot using position probability grids", *Proc. of the 14th National Conf. on Artificial Intelligence*, Portland, pp. 896-901, 1996.

[10] F. Dellaert, D. Fox, W. Burgard and S. Thrun, "Monte Carlo localization for mobile robots", *Proc. of the IEEE Int. Conf. Robotics and Automation*, Detroit, pp. 1322-1328, 1999.

[11] M. Kieffer, L. Jaulin, E. Walter and D. Meizel, "Robust autonomous robot localization using interval analysis", *Reliable Computing*, Kluwer Academic Pub., vol. 6, no. 3, pp. 337-362, 2000.

[12] A. Kelly, "Precision dilution in triangulation based mobile robot position estimation", *Proc. 8th Conference on Intelligent Autonomous Systems*, Amsterdam, 2003.

[13] J. A. Batlle, J. M. Font and J. Escoda, "Dynamic positioning of a mobile robot using a laser-based goniometer", *Proc. 5th IFAC/EURON Symposium on Intelligent Autonomous Vehicles*, Lisboa, 2004.

[14] C. D. McGillem and T. S. Rappaport, "A beacon navigation method for autonomous vehicles", *IEEE Transactions on Vehicular Technology*, vol. 38, no. 3, pp. 132-139, 1989.

[15] C. Cohen and F. Koss, "A comprehensive study of three object triangulation", *Proc. of the SPIE Conference on Mobile Robots*, Boston, pp. 95-106, 1993.

[16] M. Betke and L. Gurvits, "Mobile robot localization using landmarks", *IEEE Transactions on Robotics and Automation*, vol. 13, no. 2, pp. 251-263, 1997.

[17] C. B. Madsen and C. S. Andersen, "Optimal landmark selection for triangulation of robot position", *Robotics and Autonomous Systems*, Elsevier, vol. 23, no. 4, pp. 277-292, 1998.

[18] T. Skewis and V. Lumelsky, "Experiments with a mobile robot operating in a cluttered unknown environment", *Journal of Robotic Systems*, Wiley Pub., vol. 11, no. 9, pp. 281-300, 1994.

[19] U. D. Hanebeck and G. Schmidt, "Set theoretic localization of fast mobile robots using an angle measurement technique", *Proc. of the IEEE Int. Conference on Robotics and Automation*, Minneapolis, pp. 1387-1394, 1996.